



**Providing Choice & Value**  
Generic CT and MRI Contrast Agents



CONTACT REP

# AJNR

## **Coronal Clival Cleft in CHARGE Syndrome: Fetal MRI Series**

Sara Reis Teixeira, Carmen Cerron-Vela, Nahla Khalek,  
Renee Wright and Matthew T. Whitehead

*AJNR Am J Neuroradiol* 2025, 46 (5) 1022-1028

doi: <https://doi.org/10.3174/ajnr.A8609>

<http://www.ajnr.org/content/46/5/1022>

This information is current as  
of July 30, 2025.

# Coronal Clival Cleft in CHARGE Syndrome: Fetal MRI Series

 Sara Reis Teixeira,  Carmen Cerron-Vela, Nahla Khalek, Renee Wright, and  Matthew T. Whitehead



## ABSTRACT

**BACKGROUND AND PURPOSE:** CHARGE is a syndrome that affects the brain, eyes, ears, heart, face, and genitourinary system. Prenatal diagnosis could optimize counseling, delivery planning, and therapeutic interventions; however, reports of associated fetal neuroimaging features are scarce. While some findings are nonspecific, olfactory, inner ear, and skull base anomalies are commonly present and may be observable at the time of fetal imaging. We sought to determine the scope of prenatal CNS MRI findings in CHARGE syndrome with emphasis on findings not included in the diagnostic criteria for CHARGE syndrome, such as coronal clival cleft.

**MATERIALS AND METHODS:** Retrospective review of fetal +/- postnatal neuroimaging from patients with genetic diagnosis of CHARGE syndrome was conducted. Brain, ear, eye, face, and skull base bone abnormalities were documented. Descriptive statistics were employed to characterize the findings.

**RESULTS:** Eighteen fetal-maternal dyads were included. Median gestational age at time of prenatal MRI was 26.25 weeks. Thirteen (72%) subjects were born alive, of which 10 (55.6%) were males. One died on the first day of life (5.6%) and 4/18 (22.2%) underwent termination of pregnancy. Twelve (66.7%) had postnatal brain MRI and/or temporal bone CT. On prenatal MRI, coronal clival cleft was seen in 72% of the cases and confirmed in all patients with postnatal imaging. Inner ear dysplasia was universally seen in all prenatal MRI, except for 1 case, in which this was not evaluable, and confirmed in all cases postnatally. On prenatal imaging, olfactory apparatus hypoplasia/absence was detected in 83% of the cases, followed by globe dysmorphia and/or colobomas in 44% of the cases, atresia of choanae (39%), facial clefts (22%), and cerebellar malformation (16.7%). Of the 10 cases with postnatal brain MRI available, 4 (40%) demonstrated cerebellar gray matter heterotopia.

**CONCLUSIONS:** The most common fetal neuroimaging findings supporting the diagnosis of CHARGE syndrome are olfactory deficiency and inner ear dysplasia. Coronal clival clefts are often present and are frequently visible on prenatal MR imaging. The presence of a clival coronal cleft should raise the possibility of CHARGE syndrome, particularly when associated with other known cardinal findings, such as cerebellar dysgenesis, olfactory apparatus deficiency, and inner ear dysplasia.

**ABBREVIATIONS:** TOP = termination of pregnancy; US = ultrasound

CHARGE syndrome is a rare autosomal dominant disorder typically caused by de novo pathogenic variants in the *CHD7* (chromodomain helicase DNA-binding protein) gene, which are present in up to 65%–70% of cases.<sup>1</sup> The prevalence of CHARGE syndrome is estimated to be between 1 in 10,000 and 1 in 15,000,

depending on the region and diagnostic practices.<sup>2</sup> Blake et al<sup>3</sup> and Verloes<sup>4</sup> defined the diagnostic criteria for CHARGE syndrome based on the clinical signs and symptoms, and later in 2016, Hale et al<sup>2</sup> suggested that pathogenic *CHD7* variants should be included in the major diagnostic criteria and molecular diagnosis of CHARGE syndrome.

CHARGE is an acronym for the cardinal findings in this disorder, including ocular coloboma (C), heart defects (H), choanal atresia (A), retarded growth and/or development (R), genitourinary defects and/or hypogonadism (G), and ear anomalies and/or deafness (E). However, even though clinical diagnostic criteria have expanded over time, all features have variable expressions, and many are still nonspecific, particularly in isolation.<sup>2</sup> Clinical management depends mostly on the severity of presentations and features. For example, neonates with CHARGE syndrome can

Received August 7, 2024; accepted after revision October 17.

From the Department of Radiology (S.R.T., C.C.-V., M.T.W.), Division of Neuroradiology, The Children's Hospital of Philadelphia, Philadelphia, Pennsylvania; Perelman School of Medicine at the University of Pennsylvania (S.R.T., N.K., M.T.W.), Philadelphia, Pennsylvania; and Richard D. Wood Jr. Center for Fetal Diagnosis and Treatment at Children's Hospital of Philadelphia (N.K., R.W.), Philadelphia, Pennsylvania.

Please address correspondence to: Sara Reis Teixeira, The Children's Hospital of Philadelphia, Department of Radiology, Division of Neuroradiology, 3401 Civic Center Blvd, Philadelphia, PA 19104; e-mail: teixeiras@chop.edu

 Indicates article with supplemental data.

<http://dx.doi.org/10.3174/ajnr.A8609>

## SUMMARY

**PREVIOUS LITERATURE:** Cardinal findings in CHARGE syndrome include ocular coloboma, heart defects, choanal atresia, retarded growth and/or development, genitourinary defects, and ear anomalies. Accurate prenatal diagnosis is of utmost importance for care and counseling. Prenatal reports of head and neck and brain findings in CHARGE syndrome are scarce; most are based on ultrasound findings. Postnatally, skull base abnormalities including coronal clival cleft have been reported with high frequency, with some authors suggesting that these should be included in the diagnostic criteria for CHARGE syndrome. Nonetheless, there is a lack of fetal MRI reports of neuroimaging findings associated with CHARGE syndrome.

**KEY FINDINGS:** The most important fetal MR findings supporting the diagnosis of CHARGE syndrome include inner ear dysplasia, olfactory apparatus deficiency, and coronal clival clefts in decreasing order of frequency.

**KNOWLEDGE ADVANCEMENT:** While craniovertebral junction anomalies are not currently considered within major criteria for the diagnosis, clival clefts were present in all patients in our series and were more frequently seen on fetal MRI than other well-recognized findings in patients with CHARGE syndrome, such as ocular abnormalities or facial clefts.

have multiple life-threatening medical conditions, such as cyanosis due to congenital heart disease and choanal atresia.<sup>3</sup> Therefore, early diagnosis would be beneficial for counseling, delivery planning, and therapeutic interventions; however, reports of associated fetal neuroimaging and head and neck features are scarce; most being based on ultrasound (US) findings.<sup>1</sup> Fetal Magnetic Resonance Imaging (MRI) may add crucial information when prenatal ultrasound is suspicious. Nonetheless, the complete spectrum of neuroimaging findings associated with CHARGE syndrome that may be visible on fetal MRI is lacking in the existing medical literature.

While colobomas, inner ear dysplasia, and atresia of the choanae are standard neuroimaging features of CHARGE syndrome, other associated neuroimaging findings have been reported, including olfactory underdevelopment,<sup>5</sup> coronal clival clefts,<sup>6</sup> and cerebellar gray matter heterotopia.<sup>7</sup> Furthermore, in addition to inner ear, globe, and facial bone anomalies, olfactory and skull base abnormalities may be observable at the time of fetal imaging.<sup>6</sup> Each CHARGE-typical imaging feature that can be documented helps strengthen the diagnostic confidence for this disorder. In this study, we sought to determine the full scope of CHARGE syndrome-associated fetal brain MRI abnormalities and whether they are included in the conventional diagnostic criteria.

## MATERIALS AND METHODS

### *Study Design and Inclusion Criteria*

We performed a single-center retrospective study in a large tertiary pediatric hospital housing a fetal therapy center, where, on average, 330 fetal MRIs are performed per year. This observational study followed the STROBE guidelines. Our study was reviewed and approved by our institutional review board and complied with the Health Insurance Portability and Accountability Act (HIPAA). We obtained a waiver for documentation of informed consent. Pregnancies with suspected diagnosis of CHARGE syndrome<sup>8</sup> from 2000–2022 were considered.

Inclusion criteria were the availability of fetal MRI of the brain and confirmed genetic diagnosis of CHARGE syndrome, pre- or postnatally. Postnatal brain MRI or CT was evaluated when available. Cases were retrieved from our radiology database (mPower by Nuance Communications, and Illuminate InSight) by using the

keywords “CHARGE” and “CHARGE SYNDROME.” After excluding duplicates, we found 44 potential cases to be included. Fourteen patients were excluded because of the absence of genetic or clinical confirmatory diagnosis of CHARGE syndrome, 7 were excluded for the absence of any imaging available for review, and 5 did not have dedicated fetal brain MRI. Eighteen cases met inclusion criteria (Supplemental Data).

We obtained demographic and clinical data from the electronic chart system (Epic Systems). Gestational age at fetal MRI was calculated based on the estimated due date available in the pregnant women’s electronic medical records. Chart review was also used to supplement postnatal clinical data and confirmation of some of the imaging findings, such as presence of eye dysmorphism or colobomas, choana atresia, and facial clefts.

### *Imaging Data Acquisition*

All patients underwent either 1.5 or 3T fetal brain MRI (Siemens Medical Solutions). Slice thickness varied from 2 mm to 4 mm with an interslice gap from –1 mm to 0 mm. At the minimum, sequences performed for all patients included sagittal, coronal, and axial T2-weighted single-shot turbo spin-echo imaging. Postnatal brain MRI included at least 1 sagittal 3D T1 gradient-echo sequence (MPRAGE) with axial reformation and axial and coronal turbo spin-echo T2WI. Helically acquired CT images of the brain and/or of temporal bones were also reviewed when available.

### *Image Analysis*

Two pediatric neuroradiologists (1 with 15 years of fetal MRI experience and 1 with 2 years of experience plus 6 years of experience with pediatric radiology and fetal MRI) systematically evaluated all fetal MRI and postnatal imaging from included dyads. Prenatal and postnatal images were reviewed separately at least 2 weeks apart to avoid bias. The final data analysis was based on a consensus between the reviewers. The findings were categorized as normal, abnormal, or not evaluable. Reasons for findings to be categorized as not evaluable were variable, including motion degraded images, the low resolution of the images, lack of good in-plane images to assess the structures, lack of confidence by the reviewer(s) in determining whether a finding was

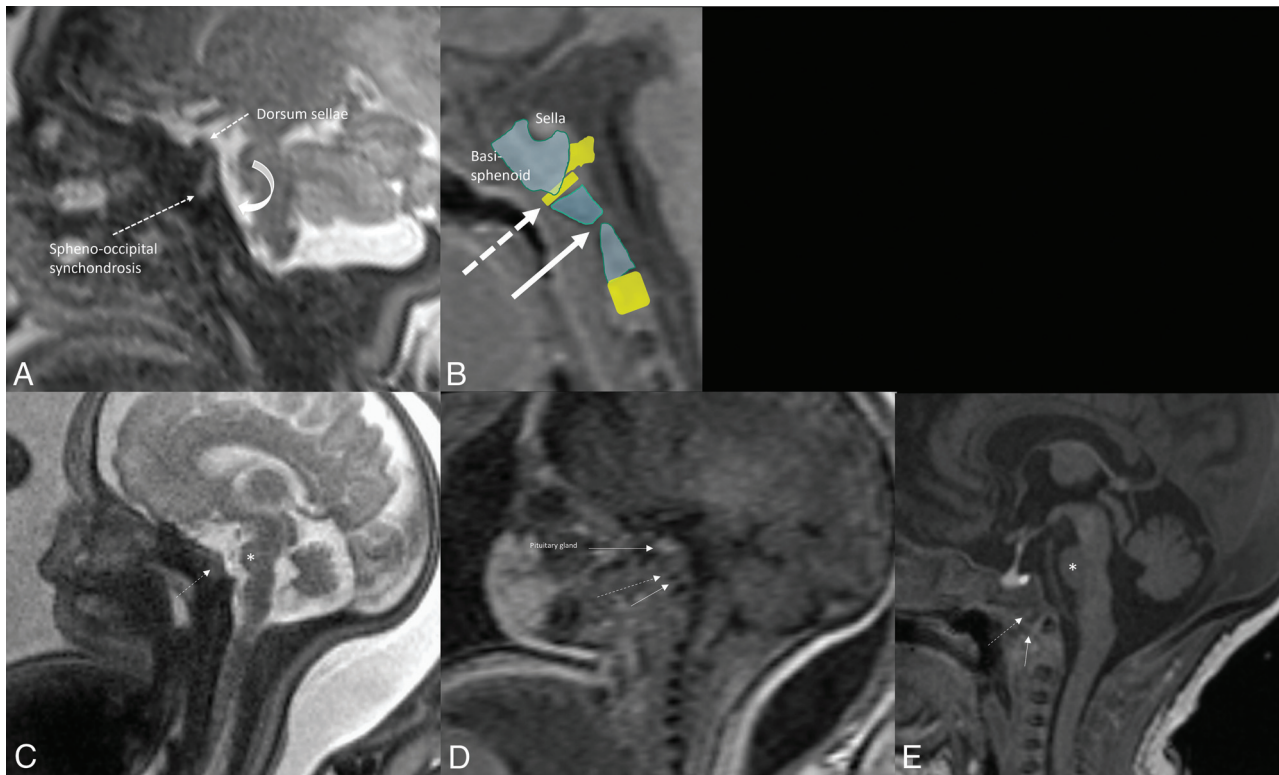


**FIG 1.** A, Parasagittal T2-weighted half-Fourier-acquired single-shot turbo spin echo (HASTE) image of a 35 weeks' gestation fetus demonstrates normal appearance of the clivus. Note the flat contour of the posterior aspect of the clivus (*curved arrow*). The dashed arrow anteriorly points to a T2 hyperintense line that corresponds to the spheno-occipital synchondrosis. B, Schematic drawing of a coronal clival cleft (*arrow*). Case c008, a 35-week gestation fetus with CHARGE syndrome (C through E). C, Parasagittal T2 HASTE and D, T1-weighted images. C, There is contour deformity of the posterior clivus suggestive of presence of clival cleft, better seen on D (*arrow*). E, Postnatal sagittal T1-weighted image of the fetus shown in C and D. Clival cleft (*arrows* in D and E). Spheno-occipital synchondrosis (*dashed arrows* in A through E). The pons (\* in C) is small in AP dimension and height, and measurements are below the 10th percentile for reported gestational age. This is better seen on postnatal imaging (E) with a disproportion of the size of the pons (\*) in relation to the midbrain and medulla oblongata. The cerebellar vermis is also small in craniocaudal and AP dimension, both on fetal and postnatal MRI.

normal or abnormal, or a combination of the aforementioned factors. The following imaging features were recorded: clivus coronal cleft, previously defined as a coronally oriented line/cleft traversing the basi-occiput of the clivus,<sup>6,9</sup> which can be incomplete (unilateral or bilateral) or complete (Fig 1); inner ear dysplasia; coloboma or dysmorphisms of the ocular globes; olfactory apparatus hypoplasia or absence; facial clefts (namely cleft lip/palate); atresia of choanae; cerebral or cerebellar malformations; ventriculomegaly; and others, including spine malformations (Fig 2). Prenatally, a coronal clival cleft may not be readily seen due to the resolution of the images. Thus, the presence of a clival cleft was suggested based on altered angulation, that is, a focally concave or other focal contour deformity of the posterior clivus (Fig 1; Supplemental Data). Prenatal inner ear dysplasia was defined as no visibility or deficiency of the cochlea and/or semicircular canals. Normal prenatal MRI appearance of the ocular globes has already been reported.<sup>10</sup> In the second trimester, the fetal globes can present with a conical configuration with angulation of the posterior contours, apex laterally eccentric, which evolves to an elliptical shape in the third trimester of gestation. Components of the hyaloid vascular system may also be seen in the early second trimester. Most fetuses have a symmetric size and appearance of

the ocular globes. On prenatal imaging, colobomas, or ocular globe dysmorphisms, were suggested when there was a marked asymmetry in size or shape of the globes, outpouching along the posterior contours of the globes centrally or slightly eccentrically located, large or small globes for reported gestational age, persistent visualization of components of the hyaloid vasculature in the third trimester, and any deviation of the expected morphology for a given gestational age. Prenatal olfactory apparatus hypoplasia or absence was defined as no visibility at the most proximal segment of the olfactory fossa.<sup>11</sup> Cerebellar malformations and the olfactory apparatus were not evaluable on postnatal temporal bone CT. The remainder of the imaging features, such as clivus coronal cleft, inner ear dysplasia, coloboma or dysmorphisms of the globes, facial clefts, atresia of choanae, and ventriculomegaly were included in the field of view and evaluable on temporal bone CT.

#### Data Analysis

Descriptive statistics were employed to characterize the findings. Continuous variables were expressed in median and range. Categorical variables were expressed in counts, proportions, and percentages. For the prenatal MRI findings, including the presence of a clival cleft, inner ear dysplasia, dysmorphisms of the ocular globes,

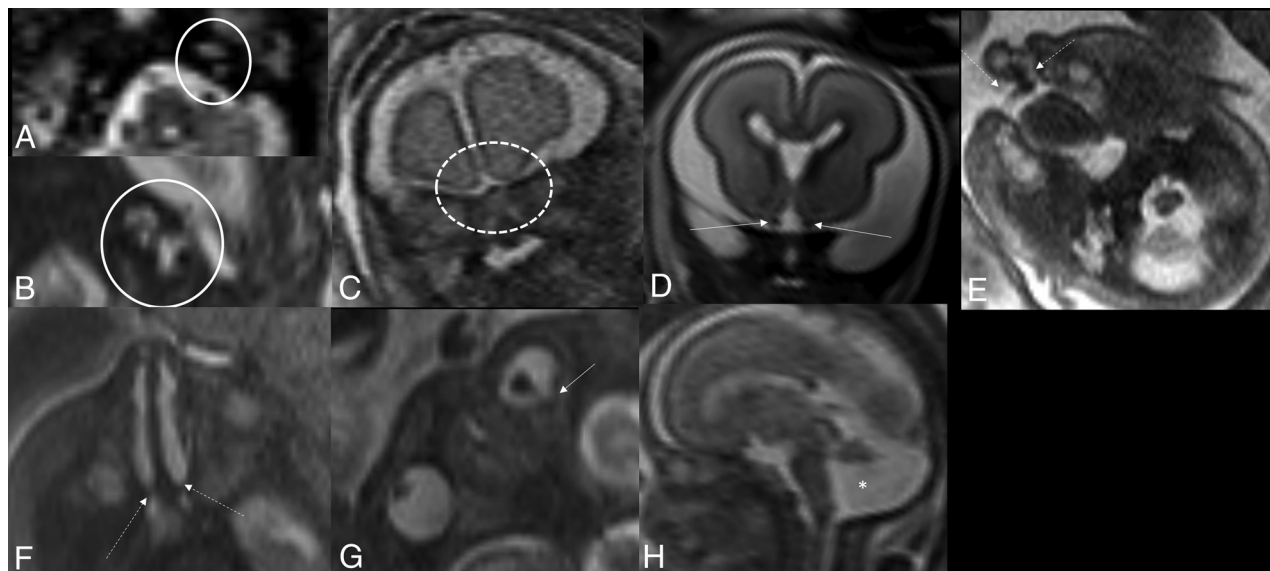


**FIG 2.** Prenatal MR neuroimaging findings in fetuses with CHARGE syndrome. A, Prenatal axial T2-weighted image of a 25.6 weeks' gestation fetus. Hypoplastic/dysplastic cochlea bilaterally (circles). The labyrinth, including semicircular canals, is not visible (not shown). Compare with normal appearance of the inner ear in a different fetus at 33 weeks' gestation (B). C, 30.6 weeks' gestation fetus. Absent olfactory apparatus on coronal T2-weighted image (dashed circle). D, For comparison, coronal T2-weighted image of a 24 weeks' gestation fetus shows T2 hypointense structures beneath the frontal lobes bilaterally consistent with the normal olfactory apparatus (arrows). E, 30.6 weeks' gestation fetus, same fetus as shown in C. Prenatal axial T2-weighted image at the level of the maxilla shows bilateral cleft palate. F, 34.1 weeks' gestation fetus, prenatal axial T2-weighted image shows atresia of choanae bilaterally (dashed arrows). G, 34 weeks' gestation fetus. Prenatal axial T2-weighted image at the level of the orbits shows bilateral eye dysmorphism with left eye coloboma (arrow) and persistent hyaloid vascular structures. Midline sagittal T2-weighted image of a 22.9 weeks' gestation fetus (H) shows hypoplastic vermis with enlarged posterior fossa consistent with Dandy-Walker malformation (\*).

olfactory apparatus hypoplasia or absence, facial clefts atresia of choanae, and cerebellar malformations, agreement and reliability (Cohen  $\kappa$ ) between readers were calculated. We also calculated agreement and reliability between prenatal and postnatal imaging findings. For the simplification of the results regarding the analysis of the pre- and postnatal findings, cases that were not evaluable were grouped together with cases with normal findings. Due to the small number of cases, sensitivity and specificity for detection of clivus cleft on prenatal MRI were not calculated. Likewise, associations between pathogenic variants and phenotype on fetal MRI were hampered because of the small number of cases.

## RESULTS

In total, 18 maternal-fetal dyads were included in our series. The Supplemental Data summarize the clinical characteristics of the dyads and specific CHD7 pathogenic variants. Eight (44.4%) were referred for central nervous system (CNS) abnormalities seen on routine obstetric US elsewhere; of those, 2 had associated complex heart disease; 4 (22.2%) were referred for gastrointestinal abnormalities 2 (11.1%) for complex heart disease and cleft lip/palate; 2 (11.1%) because of multiple congenital anomalies; 1 (5.6%) with history of prior gestation with a fetus diagnosed with CHARGE syndrome; and 1 (5.6%) fetus was found to have a chromosomal anomaly. A summary of the US findings at our fetal therapy center is also displayed in the Supplemental Data.

Fetal MRI was performed at a median gestational age of 26.25 weeks (range 20.4 to 36.3 weeks' gestation). Median maternal age at the date of the fetal was 30.5 years (range 22 to 37 years). Thirteen (72%) subjects were born alive. The remainder

of the subjects either died on the first day of life elsewhere ( $n = 1$ ; 5.6%) or underwent termination of pregnancy (TOP) ( $n = 4$ ; 22.2%). Ten (55.6%) were males, and 3 (16.7%) were females, with 5 (27.8%) subjects of unknown sex due to TOP and neonatal death. An additional 6 (33.3%) subjects died later in life; median age at postnatal death was 59 days (range 1 to 944 days) (Supplemental Data).

The main fetal MRI findings are displayed in Supplemental Data. Ten (55.6%) subjects had postnatal brain MRI, and 2 (11.1%) had only temporal bone CT. One (5.6%) subject that was born alive had no postnatal imaging available for review. Median age at postnatal imaging was 5 days (range 1 to 258 days). In the 10 cases that had postnatal imaging showing the olfactory fossa, the olfactory apparatus was correctly identified prenatally as absent in 7 cases (70%); in the remaining 3 cases (30%), it was unevaluable. For the remaining 8 prenatal cases without postnatal imaging showing the olfactory fossa, the olfactory apparatus was absent. Coronal clival cleft was confirmed in all patients with postnatal imaging, either complete in 75% of cases ( $n = 9$  of 12) or bilateral partial cleft in 25% of cases ( $n = 3$  of 12). In the 10 cases with postnatal MRI showing the cerebellum, 5 of 10 patients (50%) had cerebellar malformation of cortical development on prenatal imaging, of which 4 out of 10 (40%) demonstrated cerebellar gray matter heterotopia on postnatal imaging (Fig 3). One (10%) case presented with Dandy-Walker malformation, 3 (30%) with cerebellar hypoplasia, and only 1 case (10%) had a normal posterior fossa. All 12 cases with postnatal imaging had bilateral semicircular canal and cochlear hypoplasia.

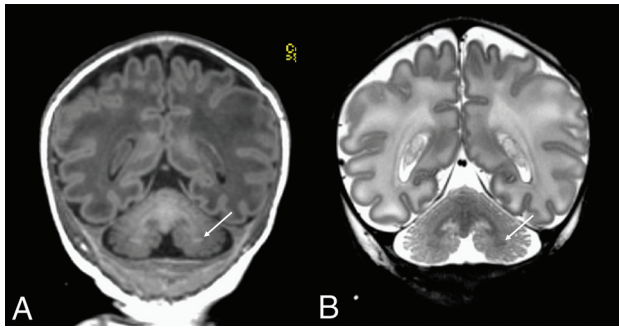


**FIG 3.** Two-day-old male, c008. Coronal T1 (A) and T2-weighted (B) images show symmetric, T1 hyperintense, and T2 hypointense foci of signal abnormality in the deep cerebellar white matter (arrows) consistent with cerebellar gray matter heterotopia.

Twelve cases had postnatal imaging showing portions of the face that included the ocular globes, nasal cavity, and palate. Of those, coloboma was found in 5 cases (42%), micro- or macropthalmia and/or eye dysmorphism in 2 cases (16%), and normal eye examination in the remaining 5 cases (42%). Choanal atresia was present in 6 (50%) of the 12 cases with postnatal imaging. Cleft lip/palate was present in 4 (33%) out of 12 cases with postnatal imaging.

Ventriculomegaly was present in 6 of the 12 cases (50%) with postnatal CNS imaging. Six (50%) patients had additional findings on MRI: Punctate foci of white matter injury, enlarged subarachnoid spaces and micrognathia, delayed myelination, subependymal cysts, peri-/intraventricular hemorrhage, dysgenesis of the corpus callosum, absent septum pellucidum, deficiency of the frontal lobes, small pons, cervical spine segmentation anomalies, and fatty filum terminale. Olfactory apparatus was absent ( $n = 8$ , 80%) or hypoplastic ( $n = 2$ , 20%) in all 10 cases with available postnatal MRI.

Discrepancies between prenatal and postnatal imaging were evaluated for 12 cases. A summary of the results is displayed in Supplemental Data. Clival cleft was correctly identified in 75% of the cases (9/12 with postnatal imaging) on prenatal MRI; 2 of the 3 remaining cases had partial clefts. Regarding the cerebellum, of the 10 cases with postnatal brain MRI, 2 cases (20%) with cerebellar malformation of cortical development and/or gray matter heterotopia were correctly identified on prenatal MRI with cerebellar vermian hypoplasia and dysmorphic folia (Supplemental Data; c005 and c007). The remaining 2 (20%) cases with cerebellar malformation of cortical development and/or gray matter heterotopia showed only cerebellar vermian hypoplasia on fetal MRI (c008 and c002). Two cases were deemed to have ventriculomegaly on fetal MRI and normal-sized ventricles on postnatal imaging (Supplemental Data; c004 and c011).

Nearly all cases with inner ear dysplasia were correctly detected on fetal MRI, except for 1 that was not evaluable. Only 2 of the 12 patients with postnatal imaging (16.7%) with macropthalmia and/or dysmorphic eyes were considered normal by fetal MRI. There were 2 (16.7%) discrepancies regarding choanal atresia: 1 patient with bilateral choanal atresia was thought to be unilateral on fetal imaging, and 1 patient with unilateral choanal atresia was considered normal on fetal MRI. All cases with facial clefts were detected on fetal MRI.

Interrater agreement and reliability in evaluating fetal MRI findings are displayed in Supplemental Data. For most of the cases, some of the discrepant results between prenatal and postnatal imaging may be potentially related to the younger gestational ages. With 1 exception, discrepancies were mostly found for fetuses <29 weeks gestation. On the contrary, for the presence of clival cleft, the major discrepancies occurred for fetuses between 29.4 and 34.1 weeks' gestation.

Fetal MRI interreader discrepancies occurred in the following gestational week age ranges: 20.4–24.6 weeks for clival clefts, 22.7–26.9 weeks for dysmorphism of the ocular globes, 21.3–24.6 weeks for inner ear dysplasia, 22.4–35.4 weeks for hypoplasia/absence of the olfactory apparatus, and 22.3–35.4 weeks for atresia of the choanae.

## DISCUSSION

We herein present fetal and postnatal neuroimaging findings from a large case series of patients with a molecular diagnosis of CHARGE syndrome. The most important fetal MR findings supporting the diagnosis of CHARGE syndrome include inner ear dysplasia, olfactory apparatus deficiency, and coronal clival clefts in decreasing order of frequency. While craniovertebral junction anomalies are not currently considered within major criteria for the diagnosis, clival clefts were present in all patients in our series and were more frequently seen on fetal MRI than other well-recognized findings in patients with CHARGE syndrome, such as ocular abnormalities or facial clefts. In addition, a detailed analysis of postnatal imaging demonstrated a high prevalence of cerebellar gray matter heterotopia, another underestimated finding.

Cephalic neural crest cells have been shown to give rise to the bones and dermal structures of the face and to induce forebrain development in the vertebrate embryo.<sup>12</sup> The mesodermal flow theory of choanal atresia by Hengerer and Strome<sup>13</sup> suggests that the excess migration of neural crest cells into the developing nasal septum and posterior choanae hinders their normal flow into the craniofacial region, which interferes with normal induction of the olfactory structures and the development of craniofacial structures, as seen in CHARGE syndrome.<sup>5</sup> It has been suggested that the *CHD7* gene encoding chromodomain helicase DNA-binding protein 7 (CHD7 protein) may play a role through the assumption of the interaction between the neural crest and somite cells, thus explaining the characteristic abnormalities seen in the olfactory bulb<sup>14</sup> and clivus,<sup>15</sup> among others.

Clival pathology is a universal feature in CHARGE syndrome. Clivus cleft, although rarely described, is a frequent finding in affected fetuses supporting this diagnosis.<sup>16</sup> Mahdi et al<sup>6</sup> reported an 87% clival cleft prevalence in their postnatal series, and suggested that coronal clival clefts should be considered an additional cardinal finding in CHARGE syndrome. Likewise, we identified coronal clival clefts on fetal MRI in up to 72% of the cases, lending further support to the notion that clival clefts should be part of the diagnostic criteria. On fetal MRI, a clival cleft is seen as either a direct linear defect or suggested by the presence of an abnormal angulation, such as a focal concave or other focal contour deformity of the posterior clivus, below the level of the sphenoparietal synchondrosis. Postnatally, it is clear and well seen as an interruption of the contours of the clivus at

the level of the basi-occiput, below the sphenoccipital synchondrosis. Defining the presence of a clival cleft is challenging on prenatal MRI and may largely depend on the image quality, expertise of the reader, and gestational age of the fetus. Clival clefts may be more visible in older fetuses; however, it is interesting to note that the major discrepancies between pre- and postnatal imaging findings regarding the presence of clival cleft occurred in the third trimester of gestation. For 2 of these cases, having a bilateral partial cleft might have posed more challenge since the midline sagittal image would show a complete bony continuity between the lower and upper moieties of the basi-occiput. The third case had a complete coronal clival cleft, which was not seen prenatally. This emphasizes how challenging it can sometimes be to detect a cleft and underscores the close attention that should be given to the fetal craniovertebral junction. In our experience, abnormal contours of the posterior aspect of the clivus are the most helpful clue in suggesting a cleft.

Other craniocervical junction abnormalities commonly reported in CHARGE syndrome, such as basilar invagination,<sup>17</sup> were not readily seen in our series. Hypoplasia of the basi-occiput may be associated with the presence of a coronal clival cleft, as seen in some of our cases (Supplemental Data), and these findings can be seen independently in different patients. Despite having thoroughly evaluated the appearance of the clivus for the presence of coronal clival cleft on fetal MRI, evaluation for hypoplasia of the clivus was not within the scope of our study.

The clivus is a central skull base bone formed by the basi-occiput and basisphenoid with the presence of a transverse sphenoccipital synchondrosis, which will ossify during adolescence in humans.<sup>18</sup> In short, after complex somitic differentiation and resegmentation, the most caudal portion of the fourth occipital somite and most rostral segment of the fifth somite will combine to form the proatlas sclerotome. Following complex signaling, the proatlas will originate the basi-occiput portion of the clivus, among other structures of the skull base and craniovertebral junction.<sup>19</sup> The coronal clival cleft rises from variations in the ossification of the basi-occiput and, therefore, has been referred to as a “basioticum variant” by some authors.<sup>19,20</sup> However, one would expect cartilaginous remnants within the cleft in this scenario. Rather, few histologic studies reported fibrous tissue separating the 2 portions of the basi-occiput in the cases of clefts.<sup>9,21,22</sup> Regardless of the embryological nature, these clefts are rare and expected to be present in association with additional craniovertebral junction and skull base abnormalities.<sup>19</sup> It should be noted that coronal clival clefts are not exclusively present in patients with CHARGE syndrome but have also been reported in cases of Cornelia de Lange syndrome,<sup>16</sup> asymptomatic patients,<sup>20</sup> and in the authors' own clinical experience, Chiari malformations and variable chromosomal disorders (not published).

In addition to the well-known cerebellar dysgenesis in patients with CHARGE syndrome, we also found that 4 out of the 10 patients with postnatal MRI demonstrated cerebellar gray matter heterotopia. Cerebellar gray matter heterotopias have been rarely reported in imaging studies. Histologically, these correspond to clusters of disorganized and normal granular cell and Purkinje neurons mixed with glial cells.<sup>7</sup> Mouse models have demonstrated reduced differentiation, proliferation, and survival of granule cell

precursors and downregulation of *Reln* in granule cells, which is required for Purkinje cell migration.<sup>23</sup> On neonatal brain MRI, these are seen as foci of T2 hypointense and T1 hyperintense signal relative to the surrounding white matter within the cerebellar hemispheres and become less conspicuous by 3 months of age, and as such, may be easily overlooked.<sup>7</sup> As reported by Wright and colleagues,<sup>7</sup> all cases with cerebellar heterotopia were associated with cerebellar hypoplasia and dysgenesis. Contrary to the high frequency of cerebellar heterotopias (up to 77% of cases) in patients with CHARGE syndrome reported by Wright and colleagues,<sup>7</sup> we suppose that the lower frequency of cerebellar heterotopias in our series may be an underestimation since some of the cases did not have MRI early enough to enable easy identification of these heterotopias. In our experience, detection of cerebellar gray matter heterotopia is beyond the resolution of fetal MRI.

In 2006, Azoulay and colleagues<sup>11</sup> showed that the olfactory sulci are always identified on MRI from 30 weeks' gestational age onwards, regardless of the MRI resolution; and that the olfactory bulbs are visible from 30 to 34 weeks' gestation. Therefore, absence of olfactory sulci/bulbs after 30 weeks could be an additional diagnostic criterion for CHARGE syndrome. Indeed, we found that the olfactory apparatus was either absent or hypoplastic in most cases and that olfactory deficiency could be identified as early as 20 gestational weeks. Almost 2 decades after Azoulay's publication, this lower age of detection is likely attributed to the enhanced resolution of state-of-the-art fetal MR imaging. Similar to our study, Blustajn and colleagues<sup>5</sup> found that olfactory abnormalities are among the most prevalent features of CHARGE syndrome. A deficiency in fibroblast growth factor signaling at the earliest stage of olfactory bulb morphogenesis in association with *CHD7* might be implicated.<sup>24</sup>

Various ear anomalies have been associated with CHARGE syndrome, including the absence of the semicircular canals, oval window atresia, and cochlear dysplasia.<sup>25</sup> In agreement with the literature, we found inner ear dysplasia in nearly all cases in our series. Based on the authors' clinical experiences, findings that are most suggestive of inner ear dysplasia on prenatal MRI are small cochlea with modiolar deficiency (absent central hypointensity on T2WI) and absent visibility of or abnormally small/dysmorphology of the semicircular canals and other labyrinthine structures.

While choanal atresia is part of the acronym and is recognized as a cardinal feature of CHARGE syndrome, this was present in only one-half of our cases.

Because of the relatively small number of maternal-fetal dyads in our series, we did not evaluate potential associations between imaging findings and genetic variant types. Similarly, estimation of the sensitivity and specificity of fetal MRI findings in the detection of features of CHARGE syndrome, particularly clival clefts, was also beyond the scope of this report. Due to the lack of results from autopsy, confirmation of some of the findings seen on prenatal imaging is hampered. We acknowledge that not all fetal structures are able to be thoroughly assessed on fetal MRI, particularly in younger fetuses. For fetuses younger than 30 weeks' gestation, it is not always possible to be certain about the status of the olfactory apparatus; hence, some cases from our study were deemed unevaluable. Inner ear dysplasia is also a challenging finding to detect on prenatal imaging. The lack of criteria for

assessing the inner ears and normal measurements of the inner ears on prenatal MRI in vivo contribute to this challenge. One of the biases of our study is that when reviewing the cases, the authors were aware of the diagnoses of CHARGE syndrome. We also did not perform a comparison with controls, so it is difficult to be certain about the weight of cognitive bias on our results.

## CONCLUSIONS

Our results demonstrate that the coronal cleft of the clivus is a characteristic finding of CHARGE syndrome, seen in high frequency on prenatal imaging and present in all cases with postnatal imaging. Inner ear dysplasia is also universally present on prenatal imaging, followed by absence or hypoplasia of olfactory apparatus, dysmorphisms of the globes, atresia of choanae, facial clefts, and cerebellar anomalies. Clival coronal clefts are either seen as direct clefts or angulation at the inner margins of the basi-occiput, below the level of the sphenoparietal synchondrosis. Presence of the clival coronal cleft should raise the possibility of CHARGE syndrome, particularly when associated with other known cardinal findings, such as cerebellar dysgenesis, hypoplasia or absence of the olfactory apparatus, and inner ear dysplasia.

Disclosure forms provided by the authors are available with the full text and PDF of this article at [www.ajnr.org](http://www.ajnr.org).

## REFERENCES

1. Traisrisilp K, Chankhunaphas W, Sittiwangkul R, et al. **Prenatal sonographic features of CHARGE syndrome.** *Diagnostics (Basel)* 2021;11:415 [CrossRef](#)
2. Hale CL, Niederriter AN, Green GE, et al. **Atypical phenotypes associated with pathogenic CHD7 variants and a proposal for broadening CHARGE syndrome clinical diagnostic criteria.** *Am J Med Genet A* 2016;170A:344–54 [CrossRef](#) [Medline](#)
3. Blake KD, Davenport SL, Hall BD, et al. **CHARGE association: an update and review for the primary pediatrician.** *Clin Pediatr (Phila)* 1998;37:159–73 [CrossRef](#) [Medline](#)
4. Verloes A. **Updated diagnostic criteria for CHARGE syndrome: a proposal.** *Am J Med Genet A* 2005;133A:306–08 [CrossRef](#) [Medline](#)
5. Blustajn J, Kirsch CFE, Panigrahy A, et al. **Olfactory anomalies in CHARGE syndrome: imaging findings of a potential major diagnostic criterion.** *AJNR Am J Neuroradiol* 2008;29:1266–69 [CrossRef](#) [Medline](#)
6. Mahdi ES, Whitehead MT. **Clival malformations in CHARGE syndrome.** *AJNR Am J Neuroradiol* 2018;39:1153–56 [CrossRef](#) [Medline](#)
7. Wright JN, Rutledge J, Doherty D, et al. **Cerebellar heterotopias: expanding the phenotype of cerebellar dysgenesis in CHARGE syndrome.** *AJNR Am J Neuroradiol* 2019;40:2154–60 [CrossRef](#) [Medline](#)
8. Sanlaville D, Verloes A. **CHARGE syndrome: an update.** *Eur J Hum Genet* 2007;15:389–99 [CrossRef](#) [Medline](#)
9. Kruff E. **Transverse cleft in the basi-occiput.** *Acta Radiology Diagn (Stockh)* 1967;6:41–48 [CrossRef](#) [Medline](#)
10. Whitehead MT, Vezina G. **Normal developmental globe morphology on fetal MR imaging.** *AJNR Am J Neuroradiol* 2016;37:1733–37 [CrossRef](#) [Medline](#)
11. Azoulay R, Fallet-Bianco C, Garel C, et al. **MRI of the olfactory bulbs and sulci in human fetuses.** *Pediatr Radiology* 2006;36:97–107 [CrossRef](#) [Medline](#)
12. Creuzet SE, Martinez S, Le Douarin NM. **The cephalic neural crest exerts a critical effect on forebrain and midbrain development.** *Proc Natl Acad Sci U S A* 2006;103:14033–38 [CrossRef](#) [Medline](#)
13. Hengerer AS, Strome M. **Choanal atresia: a new embryologic theory and its influence on surgical management.** *Laryngoscope* 1982;92:913–21 [Medline](#)
14. Pinto G, Abadie V, Mesnage R, et al. **CHARGE syndrome includes hypogonadotropic hypogonadism and abnormal olfactory bulb development.** *J Clin Endocrinol Metab* 2005;90:5621–26 [CrossRef](#) [Medline](#)
15. Nie X. **Cranial base in craniofacial development: developmental features, influence on facial growth, anomaly, and molecular basis.** *Acta Odontol Scand* 2005;63:127–35 [CrossRef](#) [Medline](#)
16. Whitehead MT, Nagaraj UD, Pearl PL. **Neuroimaging features of Cornelia de Lange syndrome.** *Pediatr Radiology* 2015;45:1198–205 [CrossRef](#) [Medline](#)
17. Fujita K, Aida N, Asakura Y, et al. **Abnormal basiocciput development in CHARGE syndrome.** *AJNR Am J Neuroradiol* 2009;30:629–34 [CrossRef](#) [Medline](#)
18. Melsen B. **Time and mode of closure of the sphenoparietal synchondrosis determined on human autopsy material.** *Acta Anat (Basel)* 1972;83:112–18 [CrossRef](#) [Medline](#)
19. Hofmann E, Prescher A. **The clivus: anatomy, normal variants and imaging pathology.** *Clin Neuroradiol* 2012;22:123–39 [CrossRef](#) [Medline](#)
20. Madeline LA, Elster AD. **Suture closure in the human chondrocranium: CT assessment.** *Radiology* 1995;196:747–56 [CrossRef](#) [Medline](#)
21. Johnson GF, Israel H. **Basioccipital clefts.** *Radiology* 1979;133:101–03 [CrossRef](#) [Medline](#)
22. Woon KC, Kokich VG, Clarren SK, et al. **Craniosynostosis with associated cranial base anomalies: a morphologic and histologic study of affected like-sexed twins.** *Teratology* 1980;22:23–35 [CrossRef](#) [Medline](#)
23. Feng W, Kawauchi D, Körkel-Qu H, et al. **Chd7 is indispensable for mammalian brain development through activation of a neuronal differentiation programme.** *Nat Commun* 2017;8:14758 [CrossRef](#) [Medline](#)
24. Dodé C, Hardelin J-P. **Kallmann syndrome: fibroblast growth factor signaling insufficiency?** *J Mol Med* 2004;82:725–34 [CrossRef](#) [Medline](#)
25. Morimoto AK, Wiggins RH, Hudgins PA, et al. **Absent semicircular canals in CHARGE syndrome: radiologic spectrum of findings.** *AJNR Am J Neuroradiol* 2006;27:1663–71 [Medline](#)